Chlamydomonas reinhardtii produces a profilin with unusual biochemical properties

David R. Kovar[1], Pinfen Yang[2], Winfield S. Sale[2], Bjørn K. Drobak[3] and Christopher J. Staiger[1,*]

[1]Department of Biological Sciences, Purdue University, West Lafayette, IN 47907-1392, USA
[2]Department of Cell Biology, Emory University School of Medicine, Atlanta, GA 30322, USA
[3]Department of Disease and Stress Biology, John Innes Centre, Norwich, NR4 7UH, UK
*Author for correspondence (e-mail: cstaiger@bilbo.bio.purdue.edu)

Accepted 13 August 2001
Journal of Cell Science 114, 4293-4305 (2001) © The Company of Biologists Ltd

SUMMARY

We report the characterization of a profilin orthologue from *Chlamydomonas reinhardtii*. CrPRF, probably the only profilin isoform, is present in both the cell body and flagella. Examination of vegetative and gametic cells by immunofluorescence microscopy using multiple fixation procedures also revealed enrichment of CrPRF at the anterior of the cell near the base of flagella and near the base of the fertilization tubule in mating type plus gametes. Purified, recombinant CrPRF binds to actin with a K_d value ~10^{-7} and displaces nuclei in a live cell 'nuclear displacement' assay, consistent with profilin's ability to bind G-actin in vivo. However, when compared with other profilin isoforms, CrPRF has a relatively low affinity for poly-L-proline and for phosphatidylinositol (4,5) bisphosphate micelles. Furthermore, and surprisingly, CrPRF inhibits exchange of adenine nucleotide on G-actin in a manner similar to human ADF or DNase I. Thus, we postulate that a primary role for CrPRF is to sequester actin in *Chlamydomonas*. The unusual biochemical properties of CrPRF offer a new opportunity to distinguish specific functions for profilin isoforms.

Key words: Actin, *Chlamydomonas*, Cytoskeleton, Mating, Profilin

INTRODUCTION

Profilin is a major regulator of actin assembly in all eukaryotic cells and profilin isoforms from angiosperm plants, vertebrates, yeasts and *Vaccinia* virus have been characterized extensively (Gibbon and Staiger, 2000; Schlüter et al., 1997). Profilin has three main cellular ligands: monomeric or G-actin, proline-rich proteins and polyphosphoinositide lipids. The formation of a 1:1 complex between profilin and G-actin can have complex effects on actin assembly. In the presence of capped filament ends, profilin functions as a simple sequestering protein, preventing actin polymerization. However, when the barbed end of filaments are not capped and a large pool of actin monomers exists, the profilin-actin complex can assemble onto F-actin. Furthermore, most profilins are able to function as nucleotide exchange factors for monomeric actin. This led to models that profilin contributes to actin assembly by 'recharging' subunits with ATP. Interestingly, plant profilins do not stimulate nucleotide exchange (Eads et al., 1998; Perelroizen et al., 1996), even with plant actin (Kovar et al., 2000a), yet still promote assembly under appropriate conditions (Perelroizen et al., 1996; Ballweber et al., 1998). Biochemical and genetic studies further underscore the concept that profilin might have distinct functions depending upon the organism in which it is found, the presence of other actin-binding proteins and other unique cellular conditions. Many questions about profilin remain, including the significance of profilin's effect on nucleotide exchange, whether profilin isoforms within the same cell perform distinct roles, whether profilin promotes polymerization or acts as a sequestering molecule during specific cellular processes and how profilin is precisely regulated by its association with other cellular ligands. Further progress on cellular roles will require continued analysis of profilin isoforms in model genetic systems (Balasubramanian et al., 1994; Cooley et al., 1992; Haarer et al., 1993; Haugwitz et al., 1994; Lu and Pollard, 2001; Wolven et al., 2000).

Chlamydomonas reinhardtii is a unicellular alga that potentially provides many experimental advantages for the study of the actin cytoskeleton and profilin. Like yeast, *Chlamydomonas* has well understood haploid genetics (Harris, 2001) and offers several molecular tools for analysis of genes and protein function (Lefebvre and Silfow, 1999). *Chlamydomonas* contains only a single conventional actin, IDA5 (Kato-Minoura et al., 1997; Sugase et al., 1996), which is predicted to be 90% identical to mammalian skeletal muscle actin, and contains an unusual, novel actin protein (Kato-Minoura et al., 1997; Lee et al., 1997). Interestingly, this novel actin can, in some instances, replace the functions of conventional actin (Kato-Minoura et al., 1997; Ohara et al., 1998). Although the localization of actin in *Chlamydomonas* has been studied (Detmers et al., 1983; Detmers et al., 1985; Harper et al., 1992), the role of the actin cytoskeleton in *Chlamydomonas* is just beginning to be understood. For example, actin has been identified as a subunit of flagellar dyneins (Kagami and Kamiya, 1992; Muto et al., 1994; Piperno and Luck, 1979; Piperno et al., 1990; Sugase et al., 1996). The role of the actin subunits in dynein is not known, but mutations in actin can lead to a failure of dynein assembly (Kato-Minoura et al., 1998). The best-understood F-actin-

containing organelle in *Chlamydomonas* is the fertilization tubule of mating type plus (mt+) gametes (Detmers et al., 1983; Detmers et al., 1985; Goodenough and Weiss, 1975; Martin and Goodenough, 1975; Wilson et al., 1997a). Defects in either the actin gene (Kato-Minoura et al., 1998) or the signal transduction events of fertilization (Pan and Snell, 2000) can result in failure to form F-actin and the fertilization tubule, thereby blocking fertilization. Finally, mutations have been identified that alter the cleavage furrow during cytokinesis, possibly by affecting the actin cytoskeleton (Ehler and Dutcher, 1998).

In interphase *Chlamydomonas* cells, little F-actin is observed (Detmers et al., 1983; Detmers et al., 1985; Harper et al., 1992), suggesting an unusual control of the actin cytoskeleton. However, actin-binding proteins that might regulate filament assembly and organization have not been reported. Here, we describe the molecular, cellular and biochemical characteristics of *Chlamydomonas* profilin, CrPRF. *CrPRF* is the only profilin gene in *Chlamydomonas*. Localization and western analysis reveals that profilin is located throughout the cell, including the flagellum, but is enriched at the anterior of the cell near the base of the flagella in vegetative and gametic cells. Biochemical characterization showed that CrPRF has a high affinity for G-actin but an extremely low affinity for both poly-L-proline and phosphatidylinositol (4,5) bisphosphate (PtdIns(4,5)P_2). Surprisingly, and in contrast to all other profilins examined, CrPRF significantly inhibits nucleotide exchange on actin. CrPRF is the first actin-binding protein characterized from *Chlamydomonas* and, based on the biochemical analysis, its primary role might be to sequester G-actin.

MATERIALS AND METHODS

Cell strains

Wild-type strains (CC-124, and CC-620 mt+) were provided by the *Chlamydomonas* Genetics Center (E. H. Harris, Duke University). CC-124, used for molecular and biochemical studies, was grown in L-medium with aeration over a 14/10 light/dark cycle (Witman, 1986). CC-620 mt+, used for immunofluorescence microscopy, was grown on L-medium agar plates.

Molecular characterization

Genomic DNA was prepared as described (Wilkerson et al., 1995). Total and poly(A)$^+$ mRNA were prepared from wild-type cells as described previously (Yang and Sale, 1998). Probes for northern- and Southern-blot analysis, and a bacterial expression construct of *Chlamydomonas* profilin, CrPRF, were produced with 30 cycles of the polymerase chain reaction (PCR) using *Pfu* DNA polymerase (Stratagene, La Jolla, CA) as described (Yang and Sale, 1998). Genomic DNA was used as a template because the predicted open reading frame did not contain introns. The sense primer (5′-ACCATGGCCTGGGAAGCCTAC-3′) introduced an *Nco*I site (underlined) into the start codon (ATG) at the 5′ end for subsequent cloning. The antisense primer (5′-CAAGTTTAGTACCCCTGGTCC-3′) included the stop codon (underlined). The resulting 400 bp product was used as a probe for northern and Southern analysis as described previously (Yang and Sale, 1998). The PCR product was cloned into the *Sma*I site in pPCRSCRIPT SK (Stratagene) following the manufacturer's instructions. The insert was then digested with *Nco*I and *Sal*I and cloned into the same sites of the pET-28a expression vector (Novagen, Madison, WI, USA). The pET-28a-CrPRF construct was transformed into strain BL21 (DE3) of *Escherichia coli*.

Protein purification

Expression of the pET-28a-CrPRF construct was induced by the addition of 0.4 mM isopropyl β-D-thiogalactopyranoside to a log-phase culture for 4 hours at 37°C. Recombinant CrPRF protein was purified by poly-L-proline (PLP)-Sepharose chromatography, according to methods described previously (Karakesisoglou et al., 1996), with modifications. Unlike other profilins we have purified, substantial amounts of CrPRF eluted from PLP-Sepharose with 1 M urea. Therefore, following washes with buffer I (20 mM Tris-HCl, 150 mM KCl, 0.2 mM DTT, pH 7.5), CrPRF was eluted with consecutive 1 M and 3 M urea washes in buffer I. The initial 1 M urea fractions were found to contain additional proteins by SDS-PAGE (not shown) and were discarded. The remaining 1 M urea eluant and entire 3 M urea eluant were pooled, yielding a 12 kDa protein. No protein contaminants were visible when 10 μg of purified protein was separated by SDS-PAGE and stained with Coomassie Blue, and yields of purified CrPRF were ~9.2 mg l^{-1} bacteria. Recombinant *Zea mays* profilin 5 (ZmPRO5) and human profilin I (HPRO1) proteins, and maize pollen actin were purified as described previously (Kovar et al., 2000a; Ren et al., 1997). Rabbit skeletal muscle actin (99% pure) was purchased from Cytoskeleton (Denver, CO, USA) and prepared with one cycle of polymerization and depolymerization as described previously (Kovar et al., 2000a). Recombinant human actin depolymerizing factor (ADF) was purified according to Hawkins et al. (Hawkins et al., 1993). Three independent batches of each profilin were used for microinjection and for the biochemical experiments described below.

Protein concentrations were determined with extinction coefficients. For ZmPRO5, A_{280}=16,000 M^{-1} cm^{-1} (Kovar et al., 2000a). For maize pollen actin and rabbit skeletal muscle actin, A_{290}=0.63 for a 1 mg ml^{-1} solution (Houk and Ue, 1974; Kovar et al., 2000a). For human profilin I, A_{280}=0.015 μM^{-1} cm^{-1}. For human ADF, A_{280}=11,210 M^{-1} cm^{-1} (Hawkins et al., 1993). An extinction coefficient (A_{280}) of 19,190 M^{-1} cm^{-1} for CrPRF was determined (Gill and von Hippel, 1989) and gave calculated protein concentrations within 5% of the concentration determined by the Bradford assay (BioRad, Hercules, CA, USA) using BSA as a standard.

Urea denaturation

The stability of the purified recombinant profilins was analysed by determining the concentration of urea required for their half-maximal denaturation, according to methods published previously (Eads et al., 1998). 1 μM profilin was incubated for 1 hour at room temperature in buffer I with increasing concentrations of urea (0-8 M). The intrinsic tryptophan fluorescence of each sample was measured with excitation at 292 nm and emission at 370 nm. Normalized relative fluorescence was then plotted versus urea concentration and fitted to a sigmoid curve.

Antisera production and analysis

Rabbit polyclonal antisera were raised (Spring Valley Laboratories, Sykesville, MD, USA) against purified recombinant CrPRF. For western analysis, a 1:5000 dilution of serum was used and purified recombinant CrPRF was used for calibration of profilin on the blots. Cell body extracts were produced by vortexing wild-type cells with glass beads and collecting the supernatant as described (Fowkes and Mitchell, 1998). Flagella, axonemes and a 0.5% Nonidet-P40-soluble fraction in Buffer A (30 mM NaCl, 10 mM Hepes, pH 7.4, 5 mM $MgSO_4$, 1 mM DTT, 0.5 mM EDTA, PMSF and aprotinin) were prepared as described previously (Yang et al., 2000). Flagellar purity was monitored by phase-contrast microscopy and isolated flagella were washed twice in buffer to avoid contamination from the cell body. To compare profilin in flagellar fractions (Fig. 3C), aliquots of flagella, axonemes and membrane matrix (detergent extract) were diluted proportionally with buffer A so that each sample was derived from equal amounts of flagella. The resulting fractions were separated on 12.5% SDS-PAGE gels. Blots were visualized by enhanced

chemiluminescence (Pharmacia Biotech, Piscataway, NJ, USA) as described previously (Yang and Sale, 1998).

For immunofluorescence, cell-wall-less mt+ vegetative cells (cw92) were grown in nitrogen-containing L-medium for three days to a final density ~2×10^6 ml^{-1}. For gametes, mt+ (cc620) and mt– (cc621) cells grown on L-plates for >6 days were resuspended in nitrogen-free M-N medium for 5 hours to induce differentiation. Gametes were activated by treatment with 15 mM dibutyryl cAMP and 0.15 mM papaverine/fresh DMSO as described (Wilson et al., 1997b) for ~40 minutes. Cells, attached to cover glasses, were processed for immunofluorescent microscopy as described (Sanders and Salisbury, 1994) with modified fixation procedures, as noted below and in the figure legend. To ensure that the localization of profilin or actin was not simply a consequence of a single method of fixation, various fixation methods were used, including 4% formaldehyde (Ted Pella, Redding, CA) in the growth medium for 10 minutes followed by 80% acetone/PBS and 100% acetone at –20°C for 6 minutes each (Fig. 4A,E) or followed by 4% formaldehyde in 0.25% Nonidet-P40 for 15 minutes (Fig. 4B). Alternatively, cells were fixed directly with 80% acetone and then with 100% acetone (Fig. 4C), or cells in suspension were fixed in 2% paraformaldehyde (Sigma, St Louis, MO, USA) for 30 minutes followed by 80% and 100% acetone fixation (Fig. 4D). Anti-CrPRF was affinity purified using recombinant CrPRF and was revealed by FITC-conjugated goat anti-rabbit antibody (ICN, Aurora, OH, USA). Actin was revealed by anti-actin monoclonal antibody C4 (ICN) and Cy5-conjugated goat anti-mouse antibody (Jackson ImmunoResearch, West Grove). Negative controls included the addition of an irrelevant primary rabbit antibody. Double labelling was recorded using confocal microscopy (Axiovert 100 M; Zeiss). FITC labelling alone was observed by inverted fluorescent light microscopy (Axiovert 35; Zeiss).

Nuclear displacement assay

Freshly opened *Tradescantia virginiana* stamen hair cells were collected and microinjected with profilin, following procedures described previously (Gibbon et al., 1997; Gibbon et al., 1998; Karakesisoglou et al., 1996; Ren et al., 1997). ~5-6 pl of protein solution was delivered into each hair cell. At least 30 cells were injected for each profilin and average times required for nuclear displacement were determined. In order to rule out the possibility that microinjection alone, or microinjection of any protein, affects the placement of the nucleus, we have previously injected equivalent concentrations of both bovine serum albumin and bovine gamma globulin (BGG) (Gibbon et al., 1997; Gibbon et al., 1998; Kovar et al., 2000a). These control injections do not cause a significant nuclear displacement during the 20 minute assay.

PLP and G-actin binding

The affinity (K_d value) of profilin for PLP was determined by measuring the increase of intrinsic tryptophan fluorescence upon complex formation (Perelroizen et al., 1994; Petrella et al., 1996), as described in detail previously (Gibbon et al., 1997; Gibbon et al., 1998). Because of the low affinity of CrPRF for PLP, solutions of 5 μM CrPRF were titrated with PLP (12 mg ml^{-1}) to a final concentration of ~6000 μM proline residues.

The ability of profilin to reduce the concentration of filamentous actin in the presence of 1 μM calcium, determined by monitoring a shift in the critical concentration (C_c) at steady state, was used to measure profilin's apparent affinity for monomeric actin, as described previously (Kovar et al., 2000a).

PtdIns(4,5)P_2-binding

PtdIns(4,5)P_2-binding was assayed by microfiltration as described previously (Haarer et al., 1993; Lambrechts et al., 1997). PtdIns(4,5)P_2 (Sigma) micelles (1 mg ml^{-1} in H_2O) were prepared by sonication for 5 minutes at room temperature. In a 150 μl reaction volume, increasing concentrations of PtdIns(4,5)P_2 (0-250 μM) micelles were incubated with 2.5 μM profilin on ice for 2 hours in 10 mM Tris-HCl, pH 7.5, 75 mM KCl, 0.5 mM DTT. The samples were then loaded onto low binding regenerated cellulose Ultrafree-MC membranes (Fisher, Pittsburgh, PA, USA) with a molecular weight cut-off of 30,000 and centrifuged for ~1 minute at 2000 ***g***. The flow-through from each reaction was separated by 15% SDS-PAGE, stained with Coomassie Brilliant Blue R (Sigma), scanned and the intensity of the profilin bands were determined with IMAGEQUANT software (Molecular Dynamics, Sunnyvale, CA, USA).

The inhibition of bean (*Vicia faba*) plasma membrane phosphoinositide phospholipase C activity by profilin was measured as described previously (Drøbak et al., 1994). Briefly, phosphoinositidase activity was assayed by incubating bean plasma membranes at 25°C in 50 μl buffer E (50 mM Tris/malate, pH 6.0, 10 μM $CaCl_2$) with 50 μM PtdIns(4,5)P_2 and 0.86 kBq ^{3}H-PtdIns(4,5)P_2, in the presence of 5 μM profilin. Reactions were stopped by the addition of 1 ml of chloroform-methanol (2:1 [v/v]). After a 5-minute incubation on ice and the addition of 250 μl of 0.6 M HCl, tubes were vortexed and centrifuged at 14,000 ***g*** for 2 minutes. 400 μl of the top phase was removed and radioactivity was determined by liquid scintillation spectrometry (Wallac 1410) after addition of scintillation fluid (Hionic-Fluor, Hewlett-Packard, UK).

Nucleotide exchange analysis

The rate of nucleotide exchange on G-actin in the absence or presence of the indicated concentrations of CrPRF, ZmPRO5, HPRO1, human ADF or DNase I (Sigma) was determined by measuring the increase in fluorescence upon incorporation of 1,N^6-ethenoadenosine 5′-triphosphate (ε-ATP; Sigma) (Goldschmidt-Clermont et al., 1992). The ε-ATP (50 μM) and profilin, ADF or DNase I (in a constant volume of 220 μl) were mixed with either 2× low salt buffer (4 mM Tris-HCl, pH 6.5, 1.0 mM DTT) or 2× physiological salt buffer (4 mM Tris-HCl, pH 7.5, 1.0 mM DTT, 200 mM KCl, 10 mM $MgCl_2$) and brought to a final reaction volume of 1.485 ml with water. The initial fluorescence was determined in a spectrofluorimeter with excitation at 360 nm and emission at 410 nm. The reaction was initiated by addition of 0.5 μM G-actin from a 50 μM stock solution in buffer G (Ren et al., 1997) and monitored for 400 seconds. The rate of ε-ATP incorporation (Δfluorescence (arbitrary units per second)) was determined by fitting the data for the first 240 seconds to a single exponential function.

The effect of a range of concentrations of CrPRF (0.1-20 μM) on the rate of nucleotide exchange of 2.0 μM pollen G-actin was carried out in low salt buffer in a similar manner. The determined rates were plotted against the concentration of CrPRF. A dissociation equilibrium constant (K_d) was calculated with MacCurveFit (Raner Software, Mt Waverly, Australia) using the equation

$$k_{obs} = k_a + (k_{ap} - k_a)\ \{[P + A + K_d] - [(P + A + K_d)^2 - 4PA]\}^{0.5} \div 4,$$

where k_a is the nucleotide exchange rate of free actin, k_{ap} is the nucleotide exchange rate of actin bound to profilin, P is the concentration of profilin and A is the concentration of actin.

RESULTS

Identification of a profilin-like gene from *Chlamydomonas reinhardtii*

While cloning the *PF24* gene from *Chlamydomonas*, we discovered an open reading frame (ORF) 860 bp upstream of the first ATG of *PF24*, a gene for an axonemal protein RSP2 (Yang and Sale, 1999). The ORF was preceded by an in-frame stop codon (TGA) 9 bp 5′ of the first ATG and a predicted TGTAA polyadenylation signal was located 330 bp 3′ of the predicted stop codon. The full nucleotide sequence information is available under GenBank accession number AF335423. A

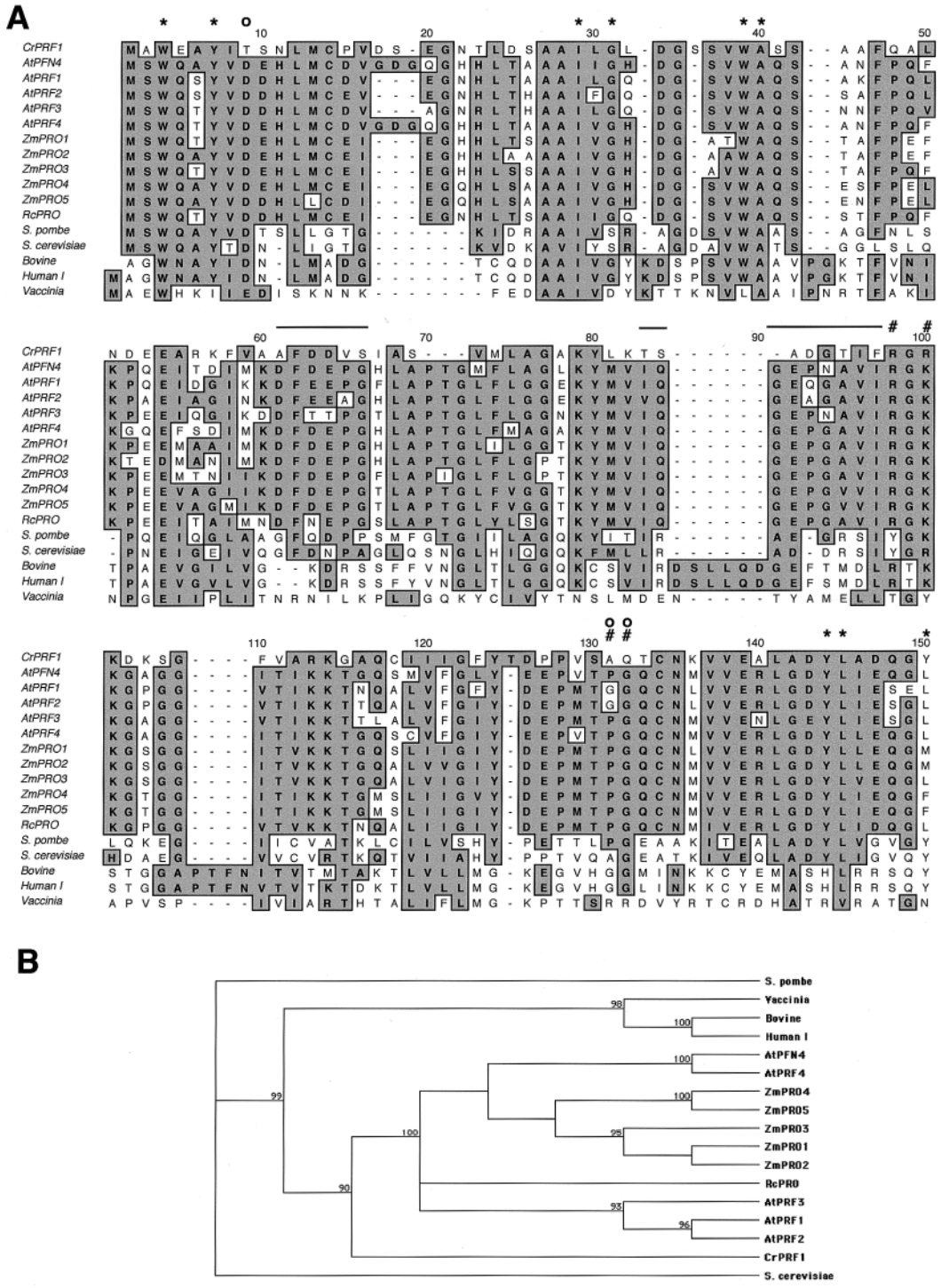

Fig. 1. Comparison of profilin amino acid sequences. (A) Multiple sequence alignment of the deduced amino acid sequence for CrPRF with plant, yeast, vertebrate and *Vaccinia* virus profilins. ClustalW analysis of the following sequences was performed using MacVector 7.0 software: *Chlamydomonas reinhardtii* (CrPRF; GenBank accession number AF335423), *Arabidopsis thaliana* profilin1 (AtPRF1; AAG10090), AtPRF2 (AAG10088), AtPRF3 (AAG10089), AtPRF4 (AAG10091), AtPFN4 (AAB39479), *Zea mays* profilin1 (ZmPRO1; X73279), ZmPRO2 (X73280), ZmPRO3 (X73281), ZmPRO4 (AF032370), ZmPRO5 (AF201459), *Ricinus communis* (RcPRO; AF092547), *Schizosaccharomyces pombe* (P39825), *Saccharomyces cerevisiae* (P07274), bovine profilin I (P02584), human profilin I (A28622) and *Vaccinia* virus profilin (P20844). Residues that are conserved in >51% of the displayed sequences are shown in bold and shaded grey. Gaps (-) were introduced to optimize the alignment. Conserved residues implicated in PLP binding are denoted by an asterisk, whereas those involved in actin binding are marked by a hash (#). The two regions of primary sequence that contribute to a plant-specific patch are overlined. Noteworthy substitutions that are predicted to affect CrPRF's association with ligands are marked with a circle. (B) Phylogenetic comparison of the profilins shown in (A). The ClustalW multiple sequence alignment was analysed with a UPGMA algorithm and bootstrapped 1000 times using MacVector 7.0 software to create the tree shown here. Similar results were obtained using an neighbour-joining algorithm (not shown).

BLAST search of the expressed sequence tag (EST) databases (NCBI; http://www.ncbi.nlm.nih.gov/) recovered several cDNA sequences that contained the entire ORF (BF866678 and AV624542) or part of the ORF. The EST nucleotide sequences were identical to the ORF and the flanking sequence except for single base pair changes in a few cases, which might be a consequence of sequencing errors or strain differences. The presence of these EST clones indicated that this ORF is an active gene.

Conceptual translation of the ORF produced a 131 amino acid long protein (Fig. 1A), with a predicted weight of 13.9 kDa and p*I* of 4.43. BLAST searches revealed that the predicted protein was orthologous to the small actin-binding protein profilin and so it was subsequently named CrPRF. CrPRF shared ~39% identity with plant profilins, ~32% identity with yeast and fungal profilins, ~23% identity with vertebrate profilins and 14% identity with *Vaccinia* virus profilin. Phylogenetic analyses placed CrPRF in a branch somewhat closer to angiosperm than to fungal profilins (Fig. 1B). Further BLAST searches of the *Chlamydomonas* EST database with the predicted amino acid sequence of CrPRF or the amino acid sequences of profilins from other organisms revealed no additional *Chlamydomonas* profilin-like isoforms. Therefore, it was predicted that this ORF encodes a bona fide profilin orthologue in *Chlamydomonas* and was likely to be the only profilin isoform.

The residues that are most highly conserved in profilins from different species are those implicated in PLP binding (Fig. 1A; Table 1); these form a hydrophobic patch positioned between the N- and C-terminal α-helices. Of 20 amino acids that are conserved in >80% of eukaryotic profilins, nine are implicated in binding to PLP and six of these make direct contact with the proline resides (Mahoney et al., 1997). All nine residues are absolutely conserved in CrPRF (Table 1). Residues that are thought to be involved in actin binding (Fig. 1A; Table 1) are less well conserved among profilins from different species (Thorn et al., 1997). Of three conserved residues, each of which makes direct contact with actin in the bovine profilin-β-actin crystal (Schutt et al., 1993), only one is conserved in CrPRF (Table 1). The phospholipid-binding site on the overall fold of eukaryotic profilins remains a matter for debate (Gibbon and Staiger, 2000; Schlüter et al., 1997) but, when a highly-conserved aspartic acid (D) on the N-terminal α-helix is changed to alanine in human (Sohn et al., 1995) or plant (Kovar et al., 2001) profilin, the resulting mutant profilins have enhanced PtdIns(4,5)P_2-binding properties. Interestingly, CrPRF contains an uncharged threonine residue at the equivalent position. Finally, examination of several plant profilin sequences and comparison of the overall fold of *Arabidopsis* profilin I and birch pollen profilin with non-plant profilin structures reveals a plant-specific patch adjacent to the actin-binding site (Fedorov et al., 1997; Thorn et al., 1997). The primary sequence of CrPRF in the equivalent region is poorly conserved, with several non-conservative substitutions and deletions. Therefore, based upon amino-acid sequence, CrPRF was predicted to have normal affinities for PLP and PtdIns(4,5)P_2, but possibly a reduced affinity for G-actin.

Table 1. Conservation of structural and functional residues shown to be identical on 80% of profilins

Residue*	Biological function‡	Conserved on CrPRF	Residue on CrPRF§
W3	PLP binding; direct contact	Yes	W3
Y6	PLP binding; direct contact	Yes	Y6
D8	Unknown; PIP_2-binding?¶	No	T8
A19	Fold conservation	Yes	A25
A20	Fold conservation	Yes	A26
I21	PLP binding	Yes	I27
G23	PLP binding	Yes	G29
W31	PLP binding; direct contact	Yes	W36
A32	PLP binding	Yes	A37
E46	Fold conservation	Yes	E49
G62	Fold conservation	No	S64
G67	Fold conservation	Yes	G69
K69	Conserved positive patch	Yes	K71
K88	Actin binding	Yes	R83
T105	Fold conservation	No	G96
G/P120	Actin binding	No	A112
G121	Actin binding	No	Q113
Y133	PLP binding; direct contact	Yes	Y125
L134	PLP binding; direct contact	Yes	L126
L/Y139	PLP binding; direct contact	Yes	L131

*Residue numbering and general scheme are after Thorn et al. (Thorn et al., 1997) for *Arabidopsis* profilin I.

‡Based on mutagenesis and/or crystal structures.

§Numbering according to Fig. 1.

¶Substitutions at this residue enhance PIP_2 binding (Sohn et al., 1995; Kovar et al., 2001).

CrPRF is a single gene in *Chlamydomonas*

To characterize the *CrPRF* gene further, Southern and northern blots were probed with the *CrPRF* coding sequence. Southern analysis of digested genomic DNA revealed fragments of predicted sizes, suggestive of a single gene (Fig. 2A). Northern analysis showed a single ~900-bp message in RNA harvested from wild-type cells (Fig. 2B). Interestingly, this message

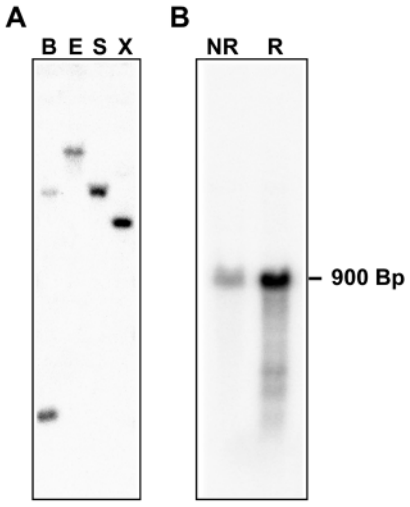

Fig. 2. *CrPRF* is the only profilin-like gene in *Chlamydomonas*. (A) Southern blot analysis of 10 μg wild-type genomic DNA digested by *Bam*HI (B), *Eco*RI (E), *Sal*I (S) or *Xho*I (X) revealed fragments of the predicted sizes, suggestive of a single *CrPRF* gene. (B) Northern blot analysis of 10 μg poly(A)$^+$ mRNA from wild-type cells (NR) or from wild-type cells collected 30 minutes after deflagellation (R). Notably, the message increased dramatically following deflagellation. The message for the *Chlamydomonas CRY* gene (Yang and Sale, 1998) was used as a loading control in all northern blots (not shown).

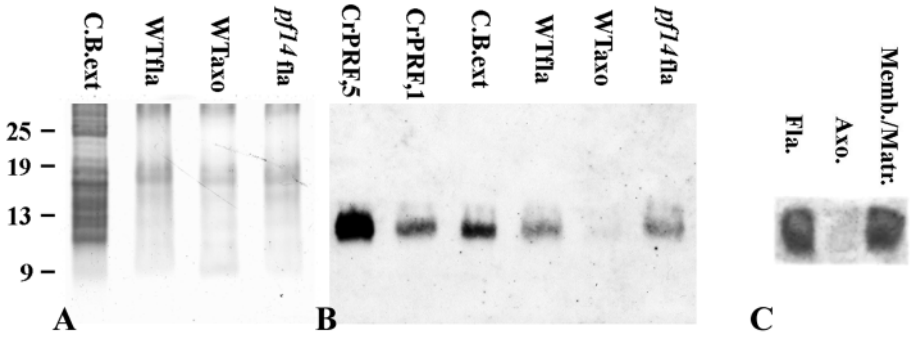

Fig. 3. Western analysis reveals CrPRF in cytoplasmic and flagellar compartments. (A,B) Coomassie Blue staining (A) and anti-CrPRF immunoblot (B) comparing cytoplasmic and flagellar fractions. (A) Each lane contained 20 μg protein from cell body extract (C.B.ext), isolated flagella from wild-type cells (WTfla), isolated axonemes from wild-type flagella (WTaxo) and isolated flagella from *pf14* cells (*pf14*fla). Molecular weight standard positions are shown on the left. (B) Lanes 3-6 are the corresponding western blots using the affinity-purified CrPRF antibody for detection. Lanes 1 and 2 were loaded with 5 ng and 1 ng purified, recombinant CrPRF. Notably, isolated flagellae contained a significant fraction of profilin (lanes 4 and 6). By contrast, axonemes contained very little profilin (lane 5). (C) Western blot comparing CrPRF in flagellar fractions. Notably, little CrPRF was found in the axoneme (Axo; lane 2). By contrast, nearly all of the flagellar CrPRF was detergent soluble and found in the membrane-matrix fraction (Memb./Matr.; lane 3).

increased dramatically when wild-type cells undergo flagellar regeneration (Fig. 2B). Upregulation of transcript expression following deflagellation is a phenomenon common to many flagellar components and suggests that CrPRF is present in the flagellar compartment. These data, along with evidence from EST database searches (see above), indicated that CrPRF is the only *Chlamydomonas* profilin isoform.

CrPRF is located in both the cytoplasm and flagella in *Chlamydomonas*

Western blot analysis using affinity-purified, CrPRF antisera revealed a single band of ~12 kDa in a cell body extract that migrated with the immunoreactive recombinant CrPRF (Fig. 3B, lanes 1-3). CrPRF was also present in the flagella (Fig. 3B) and the cell body extract and isolated flagella contained similar amounts of CrPRF (~1-5 ng per 20 μg of total protein) (Fig. 3B, lanes 1-4). These results, along with the northern analysis and immunofluorescence data shown below, strongly indicate that profilin is located in the cytoplasm and flagellum. For further subcellular analysis, flagella were fractionated into axonemes and detergent-soluble membrane-matrix fractions. Western blots of samples derived from equal amounts of flagella revealed that flagellar CrPRF was located mostly in the detergent fraction (Fig. 3C, lanes 2, 3), indicating that the flagellar fraction of profilin was not strongly associated with the axonemes. CrPRF was not reduced in the flagella of any of the motility mutants tested (Fig. 3B, lanes 4 and 6; data on other mutants not shown). We thus concluded that, in *Chlamydomonas*, CrPRF is both a cytoplasmic and flagellar component, and that the latter is soluble in detergent.

As a further test of the distribution of CrPRF, immunofluorescent localization of CrPRF and actin was carried out using affinity-purified anti-CrPRF antibody and visualized by confocal as well as wide-field fluorescence light microscopy. CrPRF is abundant throughout the cytoplasm in vegetative and gametic cells (Fig. 4A-E). Furthermore, CrPRF is enriched in two distinct, closely-opposed spots located at the anterior of the cell and adjacent to the base of the flagella (Fig. 4, arrowheads). The distinctive CrPRF spots were most prominent in cells fixed with acetone (Fig. 4C). However, the structures were visualized in all cells irrespective of fixation conditions. In contrast to CrPRF, actin was not enriched at the anterior end of vegetative cells (Fig. 4A-C). CrPRF also localized to the flagella of both vegetative (not shown owing to the plane of focus) and gametic (Fig. 4D) cells. The CrPRF-enriched spots were also located near the base of the fertilization tubule of activated mt+ gametes (Fig. 4E) and present at the anterior of mt– gametes (data not shown).

Functional characterization of CrPRF

To investigate whether CrPRF has properties similar to other profilins, recombinant CrPRF was expressed in bacteria and purified to homogeneity by PLP affinity chromatography. For direct comparison, two well-characterized profilins, recombinant *Zea mays* profilin 5 (ZmPRO5) (Kovar et al., 2000a; Kovar et al., 2001) and human profilin I (HPRO1) (Fedorov et al., 1994), were also analysed. These evolutionarily divergent profilin isoforms were characterized for their ability to bind to PLP, PtdIns(4,5)P_2 micelles and G-actin, as well as to affect the actin cytoskeleton when microinjected into the complex environment of a living cell.

The stability of bacterially expressed CrPRF was measured by urea denaturation (Fig. 5). The urea concentration required to denature half the protein (midpoint) allowed comparisons between profilin isoforms. Surprisingly, CrPRF was found to be extremely stable when compared with HPRO1 and

Table 2. Biochemical properties of *Chlamydomonas reinhardtii* profilin

Profilin	Poly-L-proline*	PtdIns(4,5)P_2‡	Nuclear displacement§
CrPRF	884±28 (6)¶	–	5.0±0.7 (30)**
ZmPRO5	164±09 (7)	–	4.8±0.7 (30)
HPRO1	328±13 (6)	+++	4.6±0.6 (34)‡‡

*Disassociation constant (K_d) values for binding to poly-L-proline are reported as μM proline residues, mean±s.d. (*n*).

‡Affinity for PtdIns(4,5)P_2 micelles is reported as the relative ability to form complex and either not pass through a microfilter or inhibit PIC activity.

§The average time in minutes (mean±s.e.m. (*n*)) required for nuclei to move outside the circumference of their original position was measured after *Tradescantia* stamen hair cells were injected with 100 μM needle concentration of protein. Injected cells were monitored for a maximum of 20 minutes.

¶The affinity of CrPRF for PLP was significantly different ($P<0.0001$) from those of both ZmPRO5 and HPRO1 by the two-tailed *t* test.

**The nuclear displacement time for CrPRF was not significantly different from those of either ZmPRO5 or HPRO1 by the two-tailed *t* test ($P=0.62$ and $P=0.83$, respectively).

‡‡Data from Gibbon et al., 1997.

ZmPRO5. Half of the recombinant HPRO1 and ZmPRO5 proteins were denatured in the presence of only 3.4±0.05 M (mean±standard deviation; n=3) and 4.0±0.06 M urea, respectively, whereas 5.2±0.06 M urea was required for half of the CrPRF to be denatured.

The affinity of CrPRF for PLP was measured by monitoring the change in intrinsic tryptophan fluorescence upon complex formation (Gibbon et al., 1997; Gibbon et al., 1998; Kovar et al., 2000a; Perelroizen et al., 1994). The average K_d value from several experiments was 884 μM proline residues (Table 2). This is an extremely low affinity compared with other profilins that have been measured and, given its extremely high protein stability, explains why CrPRF eluted from PLP-Sepharose with only 1 M urea (see Materials and Methods). By contrast, the average K_d values for ZmPRO5 and HPRO1 binding to PLP were 161 μM and 328 μM, respectively (Table 2). The affinity of CrPRF for PLP is significantly different from both ZmPRO5 and HPRO1 by the two-tailed t test (P<0.0001). Therefore, when compared with other profilins, CrPRF has an extremely low affinity for PLP.

Binding of CrPRF to PtdIns(4,5)P_2 micelles was assayed by microfiltration (Fig. 6A). When 2.5 μM HPRO1 was incubated with increasing concentrations of PtdIns(4,5)P_2 micelles, less was found to pass through a 30 kDa molecular weight cut-off filter, indicating that HPRO1 bound to the micelles to form a higher molecular weight complex. In the presence of a 25-fold (62.5 μM) excess of PtdIns(4,5)P_2, ~40% HPRO1 was found in the flow through, suggesting that 60% was in complex with PtdIns(4,5)P_2. In the presence of a 50-fold (125 μM) excess of PtdIns(4,5)P_2, no detectable HPRO1 was found in the flow through. Complete saturation of HPRO1 binding to PtdIns(4,5)P_2 at this ratio of lipid to profilin is in good agreement with previous reports using mammalian profilin I isoforms (Lambrechts et al., 1997; Lambrechts et al., 2000). Conversely, there was very little difference in the amounts of either CrPRF or ZmPRO5 found in the flow through in the absence compared with the presence of an 100-fold excess of PtdIns(4,5)P_2 (Fig. 6A).

We also investigated the association of profilin with membrane phospholipids by measuring their ability to inhibit the hydrolysis of PtdIns(4,5)P_2 by phosphoinositide-specific phospholipase C (PIC) from bean membrane (Drøbak et al., 1994) (Fig. 6B). Compared with a control without profilin, PIC activity was reduced to 48% in the presence of HPRO1. In the presence of either CrPRF or ZmPRO5, PIC activity was reduced to 78% and 76%, respectively. We had found previously that ZmPRO5 had little effect on the ability of plant phospholipase C to hydrolyse PtdIns(4,5)P_2 (Kovar et al., 2000a; Kovar et al., 2001). Together, these experiments indicated that, compared with HPRO1, CrPRF and ZmPRO5 are poor PtdIns(4,5)P_2-binding proteins.

The apparent affinities of profilin for both pollen

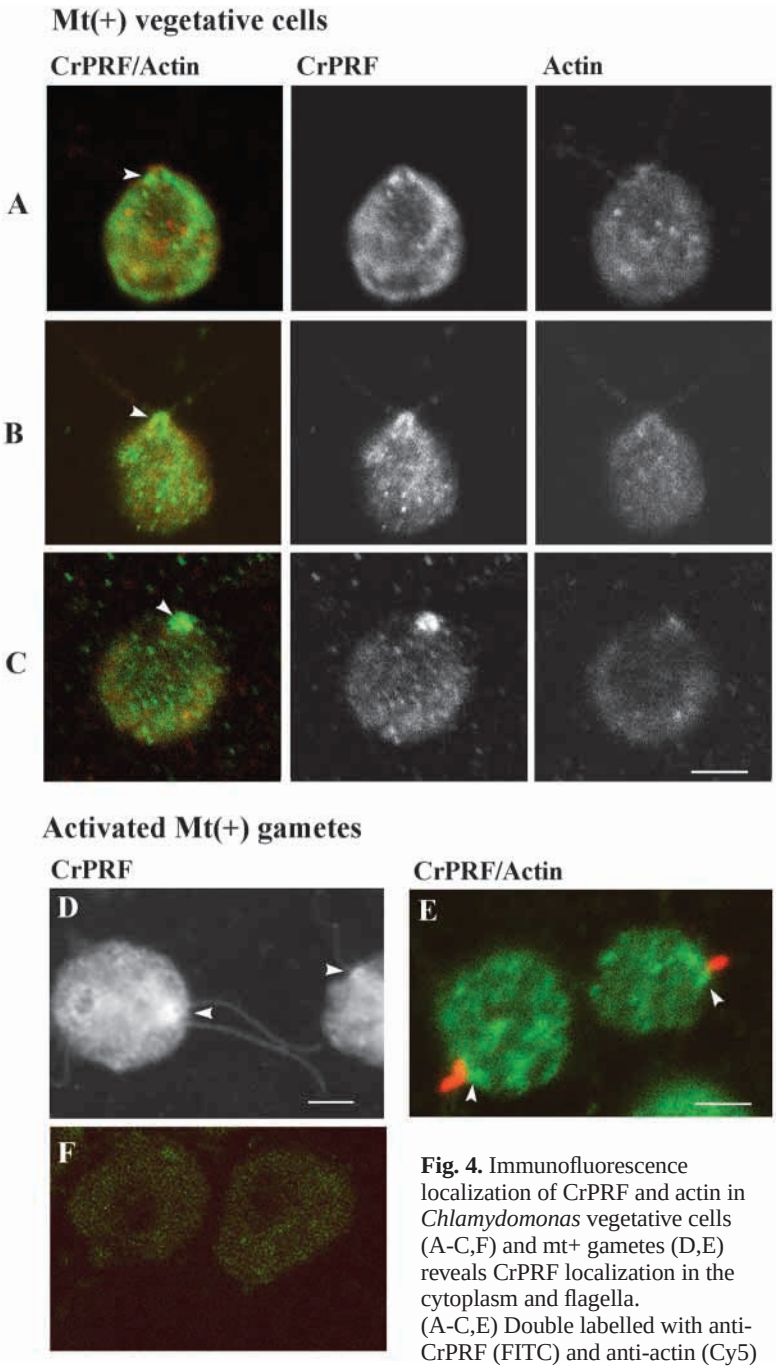

Fig. 4. Immunofluorescence localization of CrPRF and actin in *Chlamydomonas* vegetative cells (A-C,F) and mt+ gametes (D,E) reveals CrPRF localization in the cytoplasm and flagella. (A-C,E) Double labelled with anti-CrPRF (FITC) and anti-actin (Cy5) antibodies and imaged by confocal microscopy. (D-F) Single labelled and observed by wide-field fluorescence microscopy. CrPRF was relatively intensely stained throughout the cell body, including prominent staining in two CrPRF-enriched regions (A-E, arrowheads) located at the anterior end of the cells. These CrPRF-enriched regions were located at the base of the flagellae near the basal bodies and near the F-actin-containing fertilization tubule in mt+ gametes (E). The CrPRF-enriched spots were observed in all cells, irrespective of fixation condition, but staining was enhanced in cells first fixed by acetone (C). (Cells in A, B and E were first fixed in formaldehyde, cells in C and F were fixed in acetone and cells in D and F were fixed in paraformaldehyde followed by acetone.) Anti-CrPRF also stained flagellae. This is illustrated in (D) using wide-field fluorescence microscopy, and in comparison with the negative control image (F). Notably, flagellar staining was not illustrated in images A-C and E owing to the focal plane. For each image, cells selected were representative of the entire population. Scale bars, 5 μm.

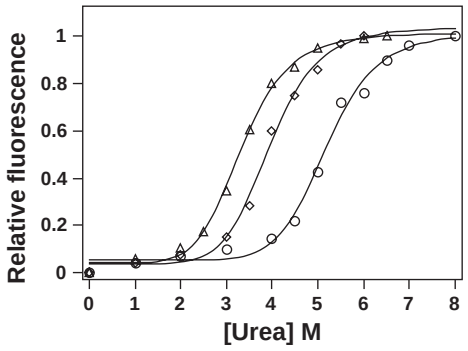

Fig. 5. CrPRF is an extremely stable profilin. The stability of CrPRF (circles), HPRO1 (triangles) and ZmPRO5 (diamonds) proteins was determined by incubating them with increasing concentrations of urea and measuring their intrinsic tryptophan fluorescences. The relative fluorescence was plotted against the urea concentration and fitted to a sigmoid curve. For this representative experiment, the denaturation midpoint for HPRO1 was 3.3 M, for ZmPRO5 4.0 M and for CrPRF 5.2 M.

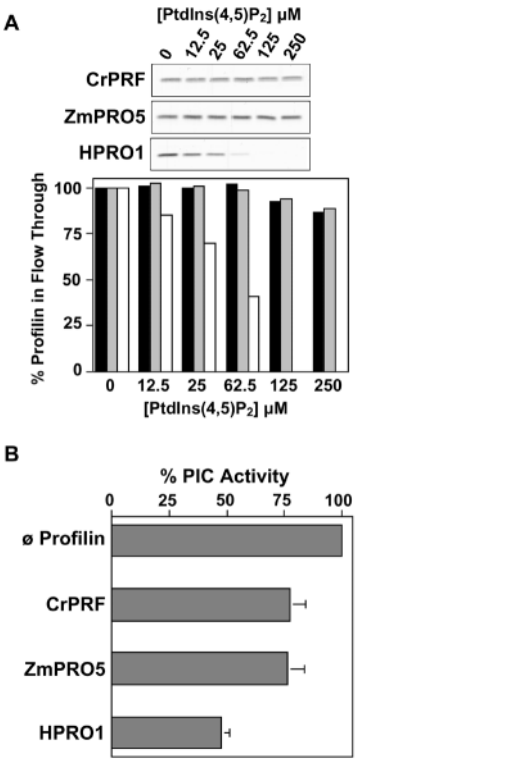

Fig. 6. CrPRF has a low affinity for PtdIns(4,5)P_2. (A) Microfiltration of profilin-PtdIns(4,5)P_2 complexes shows that little CrPRF bound to lipid micelles. The indicated concentrations of PtdIns(4,5)P_2 in micelles were incubated with 2.5 µM profilin and spun through a 30,000 molecular weight cut-off filter. The flow through was analysed by SDS-PAGE. The 14-kDa region of gels from a representative experiment are shown for CrPRF, ZmPRO5 and HPRO1 (top). The intensity of each Coomassie-stained band was determined with a densitometer and normalized against the intensity of the profilin band found in the flow through in the absence of PtdIns(4,5)P_2. Bars (bottom) represent the percentage of CrPRF (black), ZmPRO5 (grey) or HPRO1 (white) present in the flow through from two independent experiments. (B) The hydrolysis of PtdIns(4,5)P_2 by phospholipase C (PIC) was measured in the absence or presence of 5 µM profilin. Each bar represents the average (± standard deviation) of at least four independent determinations. PIC activity in the absence of profilin (ø profilin) was set to 100%.

actin and rabbit skeletal muscle actin (RSMA) were determined indirectly, by measuring the difference in the amount of filamentous actin (F-actin) in the absence, compared with the presence, of profilin. As shown in Fig. 7, increasing concentrations of G-actin alone or G-actin in the presence of 1 µM CrPRF, ZmPRO5 or HPRO1 were allowed to polymerize until steady state was reached. Subsequently, the relative amount of F-actin was determined by 90° light scattering and plotted against the starting concentration of G-actin. Using these plots and the assumptions and calculations stated previously (Kovar et al., 2000a), the apparent affinity of profilin for actin was determined. From several independent experiments, the average apparent affinities of CrPRF, ZmPRO5 and HPRO1 binding to pollen G-actin were 0.41 µM, 0.46 µM and 0.14 µM, respectively (Table 3). For ZmPRO5, these results were similar to our previous findings (Kovar et al., 2000a). The average apparent affinities of CrPRF, ZmPRO5 and HPRO1 for binding to RSMA G-actin were 0.30 µM, 0.28 µM and 0.20 µM, respectively (Table 3). For both sources of actin, CrPRF and ZmPRO5 were not significantly different from each other (P>0.25), whereas HPRO1 was significantly different from both CrPRF and ZmPRO5 for pollen actin (P<0.001) but not RSMA (P>0.2). Therefore CrPRF, ZmPRO5 and HPRO1 have similar affinities for G-actin.

To assess the interaction between CrPRF and actin further, we took advantage of an in vivo 'nuclear displacement' assay described in detail previously (Gibbon et al., 1997; Gibbon et al., 1998; Kovar et al., 2000a; Kovar et al., 2000b). The assay indirectly measures the sequestering activity of profilin by monitoring the time required for the destruction of actin filaments, indicated by the degradation of transvacuolar strands and the movement of the nucleus from a central position. As illustrated in Table 2, when CrPRF was injected, the average time for nuclear displacement was 5.0 minutes, whereas ZmPRO5 displaced the nucleus in 4.8 minutes. Previously, we found that HPRO1 displaces the nucleus in 4.6 minutes, which is similar to both ZmPRO5 and CrPRF (Gibbon et al., 1997). By contrast, *Zea mays* profilin I (ZmPRO1) displaces the nucleus significantly more slowly than these other profilins, with an average of 7.0 minutes (Gibbon et al., 1998; Kovar et

Table 3. Apparent affinities (K_d values) for rabbit skeletal muscle actin (RSMA) and maize pollen actin (MPA)

Profilin	MPA*	RSMA
CrPRF‡	0.41±0.08 (8)	0.30±0.07 (3)
ZmPRO5	0.46±0.07 (5)	0.28±0.05 (3)
HPRO1§	0.14±0.05 (4)	0.20±0.09 (3)

*The apparent K_d values for profilin binding to actin under polymerizing conditions, in the presence of 1 µM Ca^{2+}, were determined by measuring the shift in C_c values at steady state. All values, in µM, are reported as mean±s.d. (n).

‡CrPRF was not significantly different from ZmPRO5 by the two-tailed t test for either MPA or RSMA (P=0.25 and P=0.31, respectively).

§HPRO1 was significantly different from CrPRF and ZmPRO5 for MPA (P<0.001) but not for RSMA (P>0.19) by the two-tailed t test.

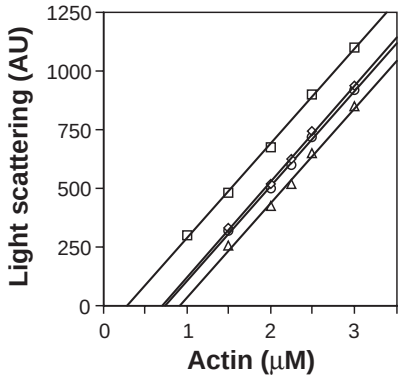

Fig. 7. CrPRF has a high apparent affinity for maize pollen G-actin. A representative experiment shows that CrPRF shifts the steady state C_c (see below) for actin assembly. Increasing concentrations of pollen G-actin were polymerized alone (squares) or in the presence of 1 μM CrPRF (circles), 1 μM ZmPRO5 (diamonds) or 1 μM HPRO1 (triangles). The *x*-axis intercepts of each regression line (C_c values) were 0.29 μM in the absence of profilin and 0.74 μM, 0.71 μM and 0.91 μM in the presence of CrPRF, ZmPRO5 and HPRO1, respectively. The calculated apparent K_d values were 0.35 μM for CrPRF1, 0.40 μM for ZmPRO5 and 0.18 μM for HPRO1. Abbreviation: A.U., arbitrary light-scattering units.

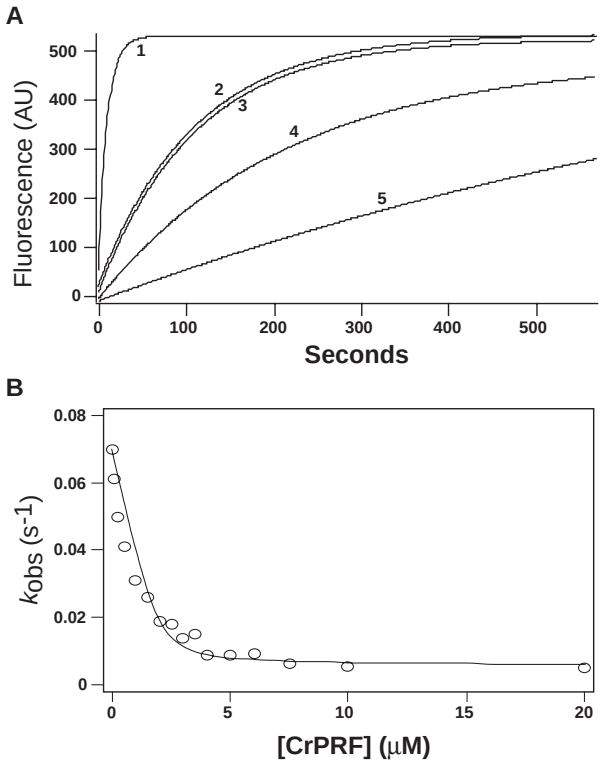

Fig. 8. CrPRF inhibits nucleotide exchange. (A) Representative experiments show that profilins from diverse organisms have substantially different effects on the initial rate of nucleotide exchange for G-actin. The incorporation of ε-ATP by 0.5 μM G-actin (RSMA) in low salt buffer alone (curve 3) or in the presence of 0.1 μM HPRO1 (curve 1), 2.5 μM ZmPRO5 (curve 2), 0.5 μM CrPRF (curve 4) or 2.5 μM CrPRF (curve 5) was monitored over time. The curves shown are fits of raw data (not shown) with a single exponential function. Human profilin I dramatically enhanced the initial rate of nucleotide exchange, whereas ZmPRO5 had little effect and CrPRF significantly decreased the initial rate. (B) The effect of a range of CrPRF concentrations (0.1-20 μM) on the initial rate of nucleotide exchange of 2.0 μM G-actin (maize pollen) in low ionic strength buffer is shown. Initial rates were determined by fitting the first 240 seconds of curves similar to those shown in (A) to a single exponential function. The initial rates were plotted against the concentration of CrPRF and fitted to the equation described in Methods. The calculated dissociation constant was 0.11 μM.

al., 2000a). Therefore, CrPRF appeared to be more similar to ZmPRO5 and HPRO1 than to ZmPRO1. The biochemical basis for differences in the live cell appears to be due primarily to differences in a profilin's apparent affinity for G-actin, because ZmPRO5, HPRO1 and CrPRF have a significantly higher affinity for G-actin than does ZmPRO1 (Kovar et al., 2000a; Kovar et al., 2001).

CrPRF inhibits the rate of nucleotide exchange on actin

Most profilins, including those from vertebrates (Goldschmidt-Clermont et al., 1992; Perelroizen et al., 1996), *Acanthamoeba* (Mockrin and Korn, 1980; Nishida, 1985), *Vaccinia* virus (Machesky et al., 1994) and yeasts (Eads et al., 1998; Lu and Pollard, 2001), have been shown to increase the exchange rate of the nucleotide bound to G-actin. However, plant profilins have no effect on nucleotide exchange (Eads et al., 1998; Perelroizen et al., 1996), even when tested with plant actin (Kovar et al., 2000a). We examined whether CrPRF behaves more similarly to plant or to non-plant profilins with respect to its effect on nucleotide exchange.

The rates of nucleotide exchange for 0.5 μM RSMA alone (Fig. 8A) and in the presence of profilin were determined by measuring the increase in fluorescence emission when G-actin incorporates the ATP analogue ε-ATP. As expected, even a substoichiometric concentration of HPRO1 (0.1 μM) significantly enhanced the rate of nucleotide exchange, whereas nearly saturating amounts of ZmPRO5 had little effect. Surprisingly, an equimolar concentration of CrPRF (0.5 μM) substantially decreased the rate of nucleotide exchange, and nearly saturating amounts of CrPRF (2.5 μM) further inhibited nucleotide exchange. To our knowledge, this is the first report of any profilin that significantly inhibits nucleotide exchange on actin.

The experiments shown in Fig. 8A were extended to include both RSMA and maize pollen actin under both low ionic and more physiological conditions. The rates of nucleotide exchange (k_{obs}, measured per second) were determined by fitting the first 240 seconds of each reaction with a single exponential function (Table 4). In the presence of either salt condition, an equal concentration of CrPRF (0.5 μM) inhibited the intrinsic rate of nucleotide exchange of both RSMA and maize pollen actin by about two times. Nearly saturating amounts of CrPRF (2.5 μM) inhibited nucleotide exchange of both actins under both conditions by four to eight times. Under all conditions tested, substoichiometric amounts of HPRO1 significantly enhanced nucleotide exchange of both actins (three to 15 times). ZmPRO5 had little effect on either source of actin under low ionic conditions, but slightly inhibited (approximately two times with nearly saturating amounts of ZmPRO5) under more physiological conditions.

For comparison with a known inhibitor of nucleotide

Table 4. Nucleotide exchange rates for rabbit skeletal muscle actin (RSMA) and maize pollen actin (MPA)

	Low ionic strength‡		Physiological§	
	RSMA	MPA	RSMA	MPA
0.5 μM actin only	0.0095±0.0005 (4)*	0.206±0.019 (4)	0.0046±0.0005 (4)	0.049±0.008 (7)
+0.5 μM CrPRF	0.0040±0.0005 (3)	0.096±0.017 (4)	0.0025±0.0003 (3)	0.020±0.004 (7)
+2.5 μM CrPRF	0.0029±0.0006 (3)	0.038±0.004 (4)	0.0012±0.0002 (3)	0.006±0.002 (7)
+0.5 μM ZmPRO5	0.0113±0.0006 (3)	0.200±0.013 (4)	0.0035±0.0005 (3)	0.033±0.004 (7)
+2.5 μM ZmPRO5	0.0110±0.0010 (3)	0.196±0.018 (4)	0.0027±0.0004 (3)	0.021±0.002 (7)
+0.1 μM HPRO1	0.1500±0.0210 (3)	0.650±0.041 (4)	0.0157±0.0006 (3)	0.162±0.010 (7)
+0.5 μM HADF	0.0049±0.0004 (3)	0.114±0.006 (4)	0.0045±0.0004 (3)	0.050±0.006 (4)
+0.5 μM DNaseI	0.0025±0.0005 (3)	0.054±0.012 (4)	0.0012±0.0003 (3)	0.025±0.001 (4)

*Nucleotide exchange rates are reported as the change in fluorescence (arbitrary units) per second±s.d. (*n*), as determined by fitting experimental data, such as those shown in Fig. 8, to a single exponential function.

‡Low ionic strength buffer: 2 mM Tris, pH 7.0, 0.5 mM DTT.

§Physiological buffer: 2 mM Tris, pH 7.5, 0.5 mM DTT, 100 mM KCl, 5 mM $MgCl_2$.

exchange, an equal concentration of human ADF (0.5 μM) inhibited nucleotide exchange of both actins by about two times under low ionic conditions (Table 4). Therefore, CrPRF and human ADF have similar effects on nucleotide exchange. Interestingly, in the presence of salt, human ADF did not appear to inhibit nucleotide exchange. An equal concentration of DNase I (0.5 μM) greatly inhibited nucleotide exchange (approximately four times) for both actins under both conditions (Table 4).

The rate of nucleotide exchange for 2 μM maize pollen actin was measured in the presence of a range of CrPRF concentrations (0.1-20 μM). Nucleotide exchange rates were plotted against the concentration of CrPRF and the data fitted to the equation described in Methods (Fig. 8B). The equilibrium dissociation constant (K_d) was determined to be 0.11 μM. This is lower than the apparent affinity derived from steady-state experiments (0.41 μM; see above).

DISCUSSION

CrPRF has an extremely low affinity for PLP and PtdIns(4,5)P_2, but a high affinity for G-actin

Profilins are ubiquitous, cytosolic proteins that form a 1:1 complex with monomeric (G-) actin and have complex effects on the actin cytoskeleton (Gibbon and Staiger, 2000; Schlüter et al., 1997). Profilins also interact with poly-L-proline and proline-rich proteins (Frazier and Field, 1997; Holt and Koffer, 2001; Wasserman, 1998), and membrane polyphosphoinositides (Lassing and Lindberg, 1985). We have described the identification and characterization of a profilin from *C. reinhardtii* (CrPRF). CrPRF protein was found in both the flagella and the cell body. Within the cell body, CrPRF is enriched in an unusual structure at the anterior end of vegetative and gametic cells at the base of the flagella. Based upon amino acid sequence comparisons with other profilins, CrPRF was predicted to have normal affinities for PLP and PtdIns(4,5)P_2 but possibly a reduced affinity for G-actin. Using two independent methods for each ligand, we discovered that CrPRF has an extremely low affinity for both PLP and PtdIns(4,5)P_2 but a high affinity for G-actin. Surprisingly, when complexed with G-actin, CrPRF inhibits nucleotide exchange strongly. To date, no other profilin has been reported to inhibit nucleotide exchange. CrPRF appears to be a unique profilin that might help to elucidate the diverse roles of profilins from evolutionarily distant species.

Numerous native and recombinant profilin isoforms have been isolated from diverse eukaryotic cells and tested for the ability to interact with the three general profilin ligands: G-actin, PLP and proline-rich peptides and phosphoinositide lipids. Direct comparison of results from these studies is complicated by differences in the approaches used by various laboratories. In general, profilins from different organisms, as well as individual profilin isoforms from the same organism, do not have identical properties. For example, three mammalian and five maize profilin isoforms are quite divergent in amino acid sequence, expression patterns and biochemical properties (Di Nardo et al., 2000; Gibbon et al., 1997; Gibbon et al., 1998; Jonckheere et al., 1999; Kovar et al., 2000a; Lambrechts et al., 1995; Lambrechts et al., 1997; Lambrechts et al., 2000; Perelroizen et al., 1996; Suetsugu et al., 1998; Witke et al., 1998). A picture emerges that, despite gross similarities in biochemical properties and overall fold, profilin isoforms might have unique functions adapted for the requirements of specific cell types.

Proline-rich binding partners are proposed to link profilin to signal transduction cascades that result in actin cytoskeleton reorganization, either through regulating the subcellular distribution or the activity of profilin (Frazier and Field, 1997; Wasserman, 1998; Holt and Koffer, 2001). The residues that are most highly conserved in profilins from different species are those implicated in PLP binding, which contribute to a hydrophobic patch positioned between the N- and C-terminal α-helices (Fedorov et al., 1997; Thorn et al., 1997). Because all nine conserved PLP-binding residues are present, we predicted that CrPRF would have a comparatively normal affinity for PLP. Affinities of profilin for PLP range from 55 μM for fission yeast profilin (Lu and Pollard, 2001) to 360 μM for human profilin (Petrella et al., 1996). Surprisingly, CrPRF has a K_d of 884 μM, which is at least a 2.5 times lower affinity for PLP than any other eukaryotic profilin measured. These results suggest that a high affinity interaction with proline-rich proteins is probably not important for the in vivo function of CrPRF. However, mammalian profilin I binds more strongly to the proline-rich protein N-WASP than does mammalian profilin II, even though profilin II has a higher affinity for PLP, demonstrating the importance of characterizing the affinity of profilins for their actual protein binding partners (Suetsugu et al., 1998).

Interaction with membrane polyphosphoinositides has also been suggested to link profilin with intracellular signalling

events (Goldschmidt-Clermont et al., 1991; Lassing and Lindberg, 1985). The phospholipid-binding site on the overall fold of profilin is still a matter of debate (Schlüter et al., 1997) but, when a highly-conserved aspartic acid on the N-terminal α-helix is changed to alanine in HPRO1 (Sohn et al., 1995) or ZmPRO5 (Kovar et al., 2001), the mutants have an increased affinity for PtdIns(4,5)P_2. CrPRF has an uncharged threonine residue at the equivalent position, which we thought might mimic the aspartic acid to alanine substitution. However, binding of CrPRF to PtdIns(4,5)P_2 micelles was barely detectable, even in the presence of a 100-fold excess of lipid. By comparison, ZmPRO5 had a similarly low affinity, whereas HPRO1 had a high affinity for PtdIns(4,5)P_2 micelles. Therefore, CrPRF does not appear to associate with membrane lipids. The possibility that CrPRF binds to D-3 phosphoinositides with higher affinity than to PtdIns(4,5)P_2, as is the case for mammalian profilin (Lu et al., 1996), should be examined.

Residues that are implicated in actin binding are poorly conserved among different profilins. Of three conserved residues that make direct contact with actin in the bovine profilin-β-actin co-crystal (Schutt et al., 1993), only one is conserved in CrPRF. However, CrPRF was found to have a high affinity for both plant G-actin (0.41 μM) and rabbit skeletal muscle G-actin (0.33 μM). Although they have been measured with different sources of actin and by a variety of methods, affinities of profilins for G-actin range from 0.1 μM to >10 μM.

The biochemical properties of CrPRF are exactly opposite from the predictions that were made based on the amino acid sequence and are not currently explainable. One possibility is that the overall fold of CrPRF is unlike those of other profilins. CrPRF is extremely stable (midpoint for denaturation is at 5.2 M urea) compared with ZmPRO5 (4.0 M), HPRO1 (3.4 M), budding yeast profilin (3.4 M) (Eads et al., 1998) and fission yeast profilin (4.5 M) (Lu and Pollard, 2001). To determine why CrPRF has unique biochemical properties, a crystal structure for CrPRF with its different ligands would be useful.

CrPRF is the only profilin known to inhibit nucleotide exchange

Because profilins inhibit the addition of monomers to the slow-growing (pointed) end but not the fast-growing (barbed) end of actin filaments (Pollard and Cooper, 1984), they can have opposite effects on the assembly of actin in vitro (Kang et al., 1999). When the barbed ends of actin filaments are capped, profilins cause depolymerization of actin filaments by binding and sequestering G-actin. Conversely, when the barbed ends are uncapped and a large pool of actin monomers is available, profilin-actin complexes can add to the barbed end and promote polymerization.

It has been suggested that profilin-enhanced polymerization involves 'recharging' ADP-loaded actin subunits with ATP, through stimulation of nucleotide exchange, because ATP-loaded G-actin adds onto filaments more readily (Goldschmidt-Clermont et al., 1992; Mockrin and Korn, 1980). Vertebrate profilin also interacts synergistically with ADF/cofilin to increase the rate of filament treadmilling 125-fold over the rate of actin alone (Didry et al., 1998). The importance of enhancing nucleotide exchange has been challenged by the fact that plant profilins do not enhance nucleotide exchange (Eads et al., 1998; Kovar et al., 2000a; Perelroizen et al., 1996), yet are still able to promote polymerization in vitro (Perelroizen et al., 1996; Ballweber et al., 1998) and interact synergistically with ADF/cofilin to increase the rate of treadmilling 75-fold over actin alone (Didry et al., 1998). The extent to which vertebrate profilin, compared with plant profilin, interacts synergistically with ADF/cofilin might be explained by its ability to enhance nucleotide exchange. Evidence for the in vivo importance of enhanced nucleotide exchange is provided for fission yeast profilin by Lu and Pollard (Lu and Pollard, 2001). A fission yeast mutant profilin with a single amino acid substitution, which does not affect actin binding but is no longer able to enhance nucleotide exchange, does not complement either profilin-null or temperature-sensitive fission yeast strains.

Therefore, profilin's ability to enhance nucleotide exchange might be important in some species (yeast), but not all (plants). Surprisingly, we found that, with near-saturating concentrations, CrPRF decreased the rate of nucleotide exchange up to eight times. The significance of this finding is not entirely clear but it certainly adds to the complexity of differences in biochemical properties between evolutionarily diverse profilins.

The intrinsic nucleotide exchange rate of actin may also be an important factor. A budding yeast actin mutation with an increased rate of nucleotide exchange suppresses defects in profilin (Wolven et al., 2000). Additionally, maize pollen actin has a 10- to 20-fold higher intrinsic rate of nucleotide exchange than rabbit skeletal muscle actin (Table 4). Perhaps plant profilins do not enhance nucleotide exchange because this is not the rate-limiting step for treadmilling in plant cells. Testing whether CrPRF complements null mutants for yeast profilin and investigating the effect of ADF/cofilin and CrPRF on the rate of filament treadmilling would be useful.

CrPRF probably functions as a G-actin-sequestering protein in *Chlamydomonas*

Actin exists predominantly in a diffuse subunit pool within the cytoplasm of *Chlamydomonas*, because interphase cells are largely devoid of phalloidin-stainable F-actin (Detmers et al., 1983; Detmers, 1985). Actin is enriched in a presumptive contractile ring structure during cytokinesis (Harper et al., 1992) and F-actin to the fertilization tubule of mt+ gametes (Detmers, 1983; Detmers, 1985). Cytochalasin treatments decrease mating efficiency by inhibiting the appearance of actin filaments in fertilization tubules, but have no obvious effect on other processes including cell division (Detmers et al., 1983; Harper et al., 1992). A mutant (*ida5*) that has complete loss of expression of the conventional *Chlamydomonas* actin gene also has no defects in cell growth or division, which might be due to compensation by a non-conventional actin (Kato-Minoura et al., 1997).

Therefore, in *Chlamydomonas*, polymeric actin appears to be required sparingly. With the exception of the CrPRF-enriched structures adjacent to the base of the flagella and underneath the fertilization tubule of mt+ gametes, CrPRF is also distributed throughout the cytosol and flagella. Although we do not know the concentration of G-actin in the cytoplasm of *Chlamydomonas*, we expect it to be higher than the critical concentration for assembly. CrPRF might be the primary actin-binding protein responsible for sequestering this pool of G-

actin. Presumably CrPRF-actin complexes are capable of assembling onto uncapped barbed ends like other profilins (Kang et al., 1999). In support of this, a direct measurement of CrPRF's affinity for G-actin gave a lower K_d value (0.11 μM) than did an indirect measurement at steady state under polymerizing conditions (0.41 μM). These differences could be due to the different ionic conditions between the two assays, or could reflect the assembly of profilin-actin complexes at steady state. Even allowing for addition of complexes onto uncapped filament ends, the apparent affinity of CrPRF for actin is high enough to account for a large amount of unpolymerized actin in the cytoplasm of interphase *Chlamydomonas* cells. To provide further evidence for this simple model, measurements of total actin, F-actin, capping protein, profilin and profilin-actin levels in *Chlamydomonas* should be made. The localization of CrPRF in flagella suggests a role in *Chlamydomonas* motility or flagellar biogenesis, perhaps by preventing undesired polymerization of actin in flagella (Kato-Minoura et al., 1997; Kato-Minoura et al., 1998; Ohara et al., 1998). CrPRF was almost entirely in the detergent-soluble fraction of flagella, suggesting that it might not interact directly with the actin subunit of the inner dynein or be involved in flagellar motility. Given the CrPRF-enriched structure at the base of the fertilization tubule of mt+ gametes, it is possible that CrPRF plays a role in actin dynamics during mating. A possible role for CrPRF in functions such as mating, cytokinesis and intraflagellar transport (Rosenbaum et al., 1999) remains to be tested.

We thank S. Almo (Albert Einstein College of Medicine) and J. Bamburg (Colorado State University) for supplying human profilin I and human ADF expression plasmids, respectively, L. Blanchoin (CNRS, Grenoble) for help fitting the nucleotide exchange data over a range of CrPRF concentrations, A. Lambrechts (Ghent University) for advice about PtdIns(4,5)P_2 microfiltration, and U. Goodenough (Washington University), N. Wilson (University of Minnesota) and S. Ono (Emory University) for advice on immunofluorescence staining. This work was supported by a US Department of Agriculture - National Research Initiative grant (99-35304-8640) to C.J.S., a grant from the National Institute of Health to P.Y. and W.S.S. and a US Department of Education GAANN training grant to D.R.K. The results reported here are in partial fulfilment of the requirements for a PhD degree by D.R.K.

REFERENCES

Balasubramanian, M. K., Hirani, B. R., Burke, J. D. and Gould, K. L. (1994). The *Schizosaccharomyces pombe cdc3*$^+$ gene encodes a profilin essential for cytokinesis. *J. Cell Biol.* **125**, 1289-1301.

Ballweber, E., Giehl, K., Hannapel, E., Huff, T., Jockusch, B. M. and Mannherz, H. G. (1998). Plant profilin induces actin polymerization from actin:β-thymosin complexes and competes directly with β-thymosins and with negative co-operativity with DNase I for binding to actin. *FEBS Lett.* **425**, 251-255.

Cooley, L., Verheyen, E. and Ayers, K. (1992). *chickadee* encodes a profilin required for intercellular cytoplasm transport during *Drosophila* oogenesis. *Cell* **69**, 173-184.

Detmers, P. A. (1985). Elongation of cytoplasmic processes during gametic mating: models for actin-based motility. *Can. J. Biochem. Cell Biol.* **63**, 599-607.

Detmers, P. A., Goodenough, U. W. and Condeelis, J. (1983). Elongation of the fertilization tubule in *Chlamydomonas*: new observations on the core microfilaments and the effect of transient intracellular signals in their structural integrity. *J. Cell Biol.* **97**, 522-532.

Detmers, P. A., Carboni, J. M. and Condeelis, J. (1985). Localization of actin in *Chlamydomonas* using antiactin and NBD-phallacidin. *Cell Motil.* **5**, 415-430.

Di Nardo, A., Gareus, R., Kwiatkowski, D. and Witke, W. (2000). Alternative splicing of the mouse profilin II gene generates functionally different profilin isoforms. *J. Cell Sci.* **113**, 3795-3803.

Didry, D., Carlier, M.-F. and Pantaloni, D. (1998). Synergy between actin depolymerizing factor/cofilin and profilin in increasing actin filament turnover. *J. Biol. Chem.* **273**, 25602-25611.

Drøbak, B. K., Watkins, P. A. C., Valenta, R., Dove, S. K., Lloyd, C. W. and Staiger, C. J. (1994). Inhibition of plant plasma membrane phosphoinositide phospholipase C by the actin-binding protein, profilin. *Plant J.* **6**, 389-400.

Eads, J. C., Mahoney, N. M., Vorobiev, S., Bresnick, A. R., Wen, K. K., Rubenstein, P. A., Haarer, B. K. and Almo, S. C. (1998). Structure determination and characterization of *Saccharomyces cerevisiae* profilin. *Biochemistry* **37**, 11171-11181.

Ehler, L. L. and Dutcher, S. K. (1998). Pharmacological and genetic evidence for a role of rootlet and phycoplast microtubules in the positioning and assembly of cleavage furrows in *Chlamydomonas reinhardtii*. *Cell Motil. Cytoskeleton* **40**, 193-207.

Fedorov, A. A., Magnus, K. A., Graupe, M. H., Lattman, E. E., Pollard, T. D. and Almo, S. C. (1994). X-ray structures of isoforms of the actin-binding protein profilin that differ in their affinity for phosphatidylinositol phosphates. *Proc. Natl. Acad. Sci. USA* **91**, 8636-8640.

Fedorov, A. A., Ball, T., Mahoney, N. M., Valenta, R. and Almo, S. C. (1997). The molecular basis for allergen cross-reactivity: crystal structure and IgE-epitope mapping of birch pollen profilin. *Structure* **5**, 33-45.

Fowkes, M. E. and Mitchell, D. R. (1998). The role of preassembled cytoplasmic complexes in assembly of flagellar dynein subunits. *Mol. Biol. Cell* **9**, 2337-2347.

Frazier, J. A. and Field, C. M. (1997). Actin cytoskeleton: are FH proteins local organizers? *Curr. Biol.* **7**, R414-R417.

Gibbon, B. G. and Staiger, C. J. (2000). Profilin. In *Actin: A Dynamic Framework For Multiple Plant Cell Functions* (ed. C. J. Staiger, F. Baluska, D. Volkmann and P. Barlow), pp. 45-65. Dordrecht, The Netherlands: Kluwer Academic Publishers.

Gibbon, B. C., Ren, H. and Staiger, C. J. (1997). Characterization of maize (*Zea mays*) pollen profilin function in vitro and in live cells. *Biochem. J.* **327**, 909-915.

Gibbon, B. C., Zonia, L. E., Kovar, D. R., Hussey, P. J. and Staiger, C. J. (1998). Pollen profilin function depends on interaction with proline-rich motifs. *Plant Cell* **10**, 981-994 [erratum: *Plant Cell* **11**, 1603].

Gill, C. G. and von Hippel, P. H. (1989). Calculation of protein extinction coefficients from amino acid sequence data. *Anal. Biochem.* **182**, 319-326.

Goldschmidt-Clermont, P. J., Kim, J. W., Machesky, L. M., Rhee, S. G. and Pollard, T. D. (1991). Regulation of phospholipase C-γ1 by profilin and tyrosine phosphorylation. *Science* **251**, 1231-1233.

Goldschmidt-Clermont, P. J., Furman, M. I., Wachsstock, D., Safer, D., Nachmias, V. T. and Pollard, T. D. (1992). The control of actin nucleotide exchange by thymosin β4 and profilin. A potential regulatory mechanism for actin polymerization in cells. *Mol. Biol. Cell* **3**, 1015-1024.

Goodenough, U. W. and Weiss, R. L. (1975). Gametic differentiation in *Chlamydomonas reinhardtii*. *J. Cell Biol.* **67**, 623-637.

Haarer, B. K., Petzold, A. S. and Brown, S. S. (1993). Mutational analysis of yeast profilin. *Mol. Cell Biol.* **13**, 7864-7873.

Harper, J. D. I., McCurdy, D. W., Sanders, M. A., Salisbury, J. L. and John, P. C. L. (1992). Actin dynamics during the cell cycle in *Chlamydomonas reinhardtii*. *Cell Motil. Cytoskeleton* **22**, 117-126.

Harris, E. H. (2001). *Chlamydomonas* as a model organism. *Annu. Rev. Plant Physiol. Plant Mol. Biol.* **52**, 363-406.

Haugwitz, M., Noegel, A. A., Karakesisoglou, J. and Schleicher, M. (1994). *Dictyostelium* amoeba that lack G-actin-sequestering profilins show defects in F-actin content, cytokinesis, and development. *Cell* **79**, 303-314.

Hawkins, M., Pope, B., Maciver, S. K. and Weeds, A. G. (1993). Human actin depolymerizing factor mediates a pH-sensitive destruction of actin filaments. *Biochemistry* **32**, 9985-9993.

Holt, M. R. and Koffer, A. (2001). Cell motility: proline-rich proteins promote protrusions. *Trends Cell Biol.* **11**, 38-46.

Houk, T. W., Jr and Ue, K. (1974). The measurement of actin concentration in solution: a comparison of methods. *Anal. Biochem.* **62**, 66-74.

Jonckheere, V., Lambrechts, A., Vandekerckhove, J. and Ampe, C. (1999). Dimerization of profilin II upon binding the $(GP_5)_3$ peptide from VASP overcomes the inhibition of actin nucleation by profilin II and thymosin β4. *FEBS Lett.* **447**, 257-263.

Kagami, O. and Kamiya, R. (1992). Translocation and rotation of microtubules caused by multiple species of *Chlamydomonas* inner-arm dynein. *J. Cell Biol.* **103**, 653-664.

Kang, F., Purich, D. L. and Southwick, F. S. (1999). Profilin promotes barbed-end actin filament assembly without lowering the critical concentration. *J. Biol. Chem.* **274**, 36963-36972.

Karakesisoglou, I., Schleicher, M., Gibbon, B. C. and Staiger, C. J. (1996). Plant profilins rescue the aberrant phenotype of profilin-deficient *Dictyostelium* cells. *Cell Motil. Cytoskeleton* **34**, 36-47.

Kato-Minoura, T., Hirono, M. and Kamiya, R. (1997). *Chlamydomonas* inner-arm dynein mutant, *ida5*, has a mutation in an actin-encoding gene. *J. Cell Biol.* **137**, 649-656.

Kato-Minoura, T., Uryu, S., Hirono, M. and Kamiya, R. (1998). Highly divergent actin expressed in a *Chlamydomonas* mutant lacking the conventional actin gene. *Biochem. Biophys. Res. Commun.* **251**, 71-76.

Kovar, D. R., Drøbak, B. K. and Staiger, C. J. (2000a). Maize profilin isoforms are functionally distinct. *Plant Cell* **12**, 583-598.

Kovar, D. R., Staiger, C. J., Weaver, E. A. and McCurdy, D. W. (2000b). AtFim1 is an actin filament-crosslinking protein from *Arabidopsis thaliana*. *Plant J.* **24**, 625-636.

Kovar, D. R., Drøbak, B. K., Collings, D. A. and Staiger, C. J. (2001). The characterization of ligand-specific maize profilin mutants. *Biochem. J.* **358**, 49-57.

Lambrechts, A., Vandamme, J., Goethals, M., Vandekerckhove, J. and Ampe, C. (1995). Purification and characterization of bovine profilin II. Actin, poly(L-proline) and inositolphospholipid binding. *Eur. J. Biochem.* **230**, 281-286.

Lambrechts, A., Verschelde, J. L., Jonckheere, V., Goethals, M., Vandekerckhove, J. and Ampe, C. (1997). The mammalian profilin isoforms display complementary affinities for PIP_2 and proline-rich sequences. *EMBO J.* **16**, 484-494.

Lambrechts, A., Braun, A., Jonckheere, V., Aszodi, A., Lanier, L., Robbens, J., Van Colen, I., Vandekerckhove, J., Fässler, R. and Ampe, C. (2000). Profilin II is alternatively spliced, resulting in profilin isoforms that are differentially expressed and have distinct biochemical properties. *Mol. Cell Biol.* **20**, 8209-8219.

Lassing, I. and Lindberg, U. (1985). Specific interaction between phosphatidylinositol 4,5-bisphosphate and profilactin. *Nature* **314**, 472-474.

Lee, V. D., Finstad, S. L. and Huang, B. (1997). Cloning and characterization of a gene encoding an actin-related protein in *Chlamydomonas*. *Gene* **197**, 153-159.

Lefebvre, P. A. and Silfow, C. D. (1999). *Chlamydomonas*: the cell and its genomes. *Genetics* **151**, 9-14.

Lu, J. and Pollard, T. D. (2001). Profilin binding to poly-L-proline and actin monomers along with ability to catalyze actin nucleotide exchange is required for viability of fission yeast. *Mol. Biol. Cell* **12**, 1161-1175.

Lu, P.-J., Shieh, W.-R., Rhee, S. G., Yin, H. L. and Chen, C.-S. (1996). Lipid products of phosphoinositide 3-kinase bind human profilin with high affinity. *Biochemistry* **35**, 14027-14034.

Machesky, L. M., Cole, N. B., Moss, B. and Pollard, T. D. (1994). Vaccinia virus expressed a novel profilin with a higher affinity for polyphosphoinositides than actin. *Biochemistry* **33**, 10815-10824.

Mahoney, N. M., Janmey, P. A. and Almo, S. C. (1997). Structure of the profilin-poly-L-proline complex involved in morphogenesis and cytoskeletal regulation. *Nat. Struct. Biol.* **4**, 953-960.

Martin, N. C. and Goodenough, U. W. (1975). Gametic differentiation in *Chlamydomonas reinhardtii*. I. Production of gametes and their fine structure. *J. Cell Biol.* **67**, 587-605.

Mockrin, S. C. and Korn, E. D. (1980). *Acanthamoeba* profilin interacts with G-actin to increase the rate of exchange of actin-bound adenosine 5′-triphosphate. *Biochemistry* **19**, 5359-5362.

Muto, E., Edamatsu, M., Hirono, M. and Kamiya, R. (1994). Immunological detection of actin in the 14S ciliary dynein of *Tetrahymena*. *FEBS Lett.* **343**, 173-177.

Nishida, E. (1985). Opposite effects of cofilin and profilin from porcine brain on rate of exchange of actin-bound adenosine 5′-triphosphate. *Biochemistry* **24**, 1160-1164.

Ohara, A., Kato-Minoura, T., Kamiya, R. and Hirono, M. (1998). Recovery of flagellar inner-arm dynein and the fertilization tubule in *Chlamydomonas ida5* mutant by transformation with actin genes. *Cell Struct. Funct.* **23**, 273-281.

Pan, J. and Snell, W. J. (2000). Signal transduction during fertilization in the unicellular green alga, *Chlamydomonas*. *Curr. Opin. Microbiol.* **3**, 596-602.

Perelroizen, I., Marchand, J.-B., Blanchoin, L., Didry, D. and Carlier, M.-F. (1994). Interaction of profilin with G-actin and poly(L-proline). *Biochemistry* **33**, 8472-8478.

Perelroizen, I., Didry, D., Christensen, H., Chua, N.-H. and Carlier, M.-F. (1996). Role of nucleotide exchange and hydrolysis in the function of profilin in actin assembly. *J. Biol. Chem.* **271**, 12302-12309.

Petrella, E. C., Machesky, L. M., Kaiser, D. A. and Pollard, T. D. (1996). Structural requirements and thermodynamics of the interaction of proline peptides with profilin. *Biochemistry* **35**, 16535-16543.

Piperno, G. and Luck, D. J. (1979). An actin-like protein is a component of axonemes from *Chlamydomonas* flagella. *J. Biol. Chem.* **254**, 2187-2190.

Piperno, G., Ramanis, Z., Smith, E. F. and Sale, W. S. (1990). Three distinct inner dynein arms in *Chlamydomonas* flagella: molecular composition and location in the axoneme. *J. Cell Biol.* **110**, 379-389.

Pollard, T. D. and Cooper, J. A. (1984). Quantitative analysis of the effect of *Acanthamoeba* profilin on actin filament nucleation and elongation. *Biochemistry* **23**, 6631-6641.

Ren, H., Gibbon, B. C., Ashworth, S. L., Sherman, D. M., Yuan, M. and Staiger, C. J. (1997). Actin purified from maize pollen functions in living plant cells. *Plant Cell* **9**, 1445-1457.

Rosenbaum, J. L., Cole, D. G. and Diener, D. R. (1999). Intraflagellar transport: the eyes have it. *J. Cell Biol.* **144**, 385-388.

Sanders, M. A. and Salisbury, J. L. (1994). Immunofluorescence microscopy of cilia and flagella. *Methods Cell Biol.* **47**, 163-169.

Schlüter, K., Jockusch, B. M. and Rothkegel, M. (1997). Profilins as regulators of actin dynamics. *Biochim. Biophys. Acta* **1359**, 97-109.

Schutt, C. E., Myslik, J. C., Rozycki, M. D., Goonesekere, N. C. W. and Lindberg, U. (1993). The structure of crystalline profilin-β-actin. *Nature* **365**, 810-816.

Sohn, R. H., Chen, J., Koblan, K. S., Bray, P. F. and Goldschmidt-Clermont, P. J. (1995). Localization of a binding site for phosphatidylinositol-4,5-bisphosphate on human profilin. *J. Biol. Chem.* **270**, 21114-21120.

Suetsugu, S., Miki, H. and Takenawa, T. (1998). The essential role of profilin in the assembly of actin for microspike formation. *EMBO J.* **17**, 6516-6526.

Sugase, Y., Hirono, M., Kindle, K. L. and Kamiya, R. (1996). Cloning and characterization of the actin-encoding gene of *Chlamydomonas reinhardtii*. *Gene* **168**, 117-121.

Thorn, K. S., Christensen, H. E. M., Shigeta, R., Huddler, D., Shalaby, L., Lindberg, U., Chua, N. H. and Schutt, C. E. (1997). The crystal structure of a major allergen from plants. *Structure* **5**, 19-32.

Wasserman, S. (1998). FH proteins as cytoskeletal organizers. *Trends Cell Biol.* **8**, 111-115.

Wilkerson, C. G., King, S. M., Koutoulis, A., Pazour, G. J. and Witman, G. B. (1995). The 78,000 M_r intermediate chain of *Chlamydomonas* outer arm dynein is a WD-repeat protein required for arm assembly. *J. Cell Biol.* **129**, 169-178.

Wilson, N. F., Figkesib, M. J. and Snell, W. J. (1997a). The *Chlamydomonas* mating type plus fertilization tubule, a prototypic cell fusion organelle: isolation, characterization, and in vitro adhesion to mating type minus gametes. *J. Cell Biol.* **137**, 1537-1553.

Wilson, N. F., Foglesong, M. J. and Snell, W. J. (1997b). The *Chlamydomonas* mating type plus fertilization tubule, a prototypic cell fusion organelle: isolation, characterization, and in vitro adhesion to mating type minus gametes. *J. Cell Biol.* **137**, 1537-1553.

Witke, W., Podtelejnikov, A. V., Di Nardo, A., Sutherland, J. D., Gurniak, C. B., Dotti, C. and Mann, M. (1998). In mouse brain profilin I and profilin II associate with regulators of the endocytic pathway and actin assembly. *EMBO J.* **17**, 967-976.

Witman, G. B. (1986). Isolation of *Chlamydomonas* flagella and flagellar axonemes. *Methods Enzymol.* **134**, 280-290.

Wolven, A. K., Belmont, L. D., Mahoney, N. M., Almo, S. C. and Drubin, D. G. (2000). In vivo importance of actin nucleotide exchange catalyzed by profilin. *J. Cell Biol.* **150**, 895-903.

Yang, P. and Sale, W. S. (1998). The M_r 140,000 intermediate chain of *Chlamydomonas* flagellar inner arm dynein is a WD-repeat protein implicated in dynein arm anchoring. *Mol. Biol. Cell* **9**, 3335-3349.

Yang, P. and Sale, W. S. (1999). Flagellar radial spoke protein 2 (RSP2) is a protein kinase. *Mol. Biol. Cell* **10**, 338a.

Yang, P., Fox, L., Colbran, R. J. and Sale, W. S. (2000). Protein phosphatases PP1 and PP2A are located in distinct positions in the *Chlamydomonas* flagellar axoneme. *J. Cell Sci.* **113**, 91-102.